

Effects of a 300 mT Static Magnetic Field on Human Umbilical Vein Endothelial Cells

Lucia Potenza,^{1*} Chiara Martinelli,¹ Emanuela Polidori,¹ Sabrina Zeppa,¹ Cinzia Calcabrini,¹
Laura Stocchi,² Piero Sestili,¹ and Vilberto Stocchi¹

¹*Dipartimento di Scienze Biomolecolari, Università degli Studi di Urbino "Carlo Bo", Urbino, Italy*

²*U.O.C. Genetica Medica, Fondazione Policlinico Tor Vergata, Rome, Italy*

This study describes the effects of a static magnetic field (SMF) on cell growth and DNA integrity of human umbilical vein endothelial cells (HUVECs). Fast halo assay was used to investigate nuclear damage; quantitative polymerase chain reaction (QPCR), standard PCR, and real-time PCR were used to evaluate mitochondrial DNA integrity, content, and gene expression. HUVECs were continually exposed to a 300 mT SMF for 4, 24, 48, and 72 h. Compared to control samples (unexposed cultures) the SMF-exposed cells did not show a statistically significant change in their viability. Conversely, the static field was shown to be significant after 4 h of exposure, inducing damage on both the nuclear and mitochondrial levels, reducing mitochondrial content and increasing reactive oxygen species. Twenty-four hours of exposure increased mitochondrial DNA content as well as expression of one of the main genes related to mitochondrial biogenesis. No significant differences between exposed and sham cultures were found after 48 and 72 h of exposure. The results suggest that a 300 mT SMF does not cause permanent DNA damage in HUVECs and stimulates a transient mitochondrial biogenesis. Bioelectromagnetics © 2010 Wiley-Liss, Inc.

Key words: static magnetic field; DNA damage; mitochondrial biogenesis; mitochondrial DNA; nuclear DNA

INTRODUCTION

In the last few years, the increasing production of electromagnetic and static magnetic fields (EMFs and SMFs, respectively), due to the expanding use of electronic devices in everyday life, has led to a number of studies on the effects of these fields on living organisms [Hong, 1995; Dini and Abbro, 2005; Miyakoshi, 2006; Dini et al., 2009]. However, fewer studies have been conducted on SMFs than on EMFs.

The growing interest in the influence of SMFs on life processes may also stem from the increasing use of these fields as therapeutic and diagnostic instruments (e.g., magnetic resonance imaging and coupling of magnetic field (MF) exposure with chemotherapy) [Kheifets, 2001; Xu et al., 2001; Karasek and Lerchl, 2002; Dini and Abbro, 2005; Nursal et al., 2006; Franco et al., 2008; Henry et al., 2008; Rumbaut and Mirkovic, 2008; Strelczyk et al., 2009]. In order to research the biological effects of SMFs on living systems, SMFs are usually classified as weak (<1 mT), moderate (1 mT to 1 T), strong (1–5 T), and ultrastrong (>5 T) [Dini and Abbro, 2005].

SMFs have a variety of effects on living organisms ranging from an enhanced rate of enzymatic reactions to increased transcription levels and alterations in cellular

growth [Cairo et al., 1998; Katsir and Parola, 1998; Katsir et al., 1998; Ishizaki et al., 2001]. Moreover, SMF bioeffects are stronger when applied in combination with other external factors such as ionizing radiation and certain chemicals [Zmyslony et al., 2000; Sabo et al., 2002]; for example, SMFs were found to enhance the *in vivo* action of adriamycin, a chemotherapeutic agent, against transplanted mammary tumors in mice [Gray et al., 2000].

The data reported in literature are quite heterogeneous in terms of SMF intensity (from 10^{-7} to 10 T), subjects exposed (from various cultured cells to humans) and exposure times (from minutes to months), so it is difficult to compare them directly and a clear evaluation cannot yet be made [Dini and Abbro, 2005;

Grant sponsor: Research Grant at Pharmacy Faculty of Urbino.
*Correspondence to: Lucia Potenza, Dipartimento di Scienze Biomolecolari, Università degli Studi di Urbino "Carlo Bo", Via A. Saffi, 2, 61029 Urbino, Italy. E-mail: lucia.potenza@uniurb.it

Received for review 21 October 2009; Accepted 8 May 2010

DOI 10.1002/bem.20591
Published online in Wiley InterScience
(www.interscience.wiley.com).

Miyakoshi, 2005]. Hence, our present knowledge of the effects of SMFs on living organisms is still very limited. In particular, little is known about the effects of SMFs on the mitochondria, which play an important role in biological systems [Dini et al., 2009].

In order to gain insight into the effects of SMFs on these important organelles, we carried out a study in which we directly tested the effect of a 300 mT SMF on a cellular level in human umbilical vein endothelial cells (HUVECs). Cell growth, nuclear (n), and mitochondrial (mt) DNA damage, mitochondrial content and reactive oxygen species (ROS) production were investigated after 4, 24, 48, and 72 h of SMF exposure.

A 300 mT SMF was chosen because we have an ongoing interest in how biological systems respond to SMF at mT levels [Potenza et al., 2004]. Further investigation in this field strength is also useful because of potential SMF therapy applications in the treatment of vascular and circulatory disease, including ischemic pain and hypertension [Okano et al., 2006; Okano, 2008]. In this direction, the use of HUVECs as a cell model may contribute to the understanding of the interaction between moderate MFs and endothelial cells, and may allow the design of new vascular therapies. Furthermore, these cells are among the first line of defense against environmental stress including SMFs.

MATERIALS AND METHODS

Magnetic Field Application

SMFs were produced by neodymium magnetic disks (28.85 mm diameter and 10 mm thickness) provided by Calamit Trading (Cologno Monzese, Italy). The system used has been reported by Potenza et al. [2004]. The magnets were inserted into slits carved on a polystyrene plate and placed under the cell culture dishes (35 mm) at a distance greater than 10 cm. At this distance the MF of the magnet is extremely low. The MF was oriented vertically, with the north pole at the bottom. The magnitude of the MF in the test cultures was determined by means of a Hall-effect probe magnetometer (GM04, Hirst Magnetic Instruments, Falmouth, Cornwall, UK). In the control conditions cells were fixed like the exposed cells but without the magnets. Both the exposed and control samples were kept in the same incubator at 37 °C. The magnets did not produce temperature variation as shown by repeated temperature checks throughout the incubator.

A Faraday shield for the entire incubator protected against any electrical disturbance. The cultures to be exposed were placed in the upper left part of the incubator, whereas the control cultures were placed in

the lower right, at a distance at which the MF was many orders of magnitude lower (measured by the same probe magnetometer).

All experiments were carried out with magnets that produced a peak strength of 300 mT in the middle of the culture dish. For this type of exposure, natural variations of terrestrial MFs were not taken into account because of their negligible intensity compared with the applied MF. An environmental monitoring of MFs (in the range of 0–100 Hz) from some unknown source was conducted using the previously mentioned probe many days before, during and after the experimental tests and showed no detectable fields inside the apparatus. It was concluded that the environmental field variation as a function of time was too small to be measured (below 10^{-4} mT).

All the experiments were carried out on cell samples after 4, 24, 48, and 72 h of incubation in the presence or absence of SMF.

Cell Culture and Static Magnetic Field Exposure

HUVECs were cultured at 37 °C in an atmosphere of 95% air and 5% CO₂ in M199 medium (B-48800; Lonza, Verviers, Belgium) containing antibiotics, 1.4 mM glutamine, 10% fetal bovine serum, and 50 µg/ml endothelial cell growth factor. HUVECs were seeded at an appropriate density 30–36 h before treatments. At the SMF exposure stage, the cell number was 10^5 cells/well. After the exposure, cells were washed with phosphate-buffered saline (PBS, 8 g/L NaCl, 1.15 g/L Na₂HPO₄, 0.2 g/L KH₂PO₄, 0.2 g/L KCl), harvested by trypsinization and processed for DNA damage analyses or viability studies, or recultured in the original medium at different times (5 and 24 h) for mitochondrial activity studies.

Trypan Blue Exclusion Assay

Following SMF exposure (4, 24, 48, and 72 h) monolayers were detached by trypsinization; an aliquot of cell suspension was diluted 1:1 with 0.4% trypan blue, and cells were counted with a hemocytometer. Results were expressed as the absolute number of viable (unstained) cells in treated versus untreated samples. Five separate determinations, each in duplicate, were performed. The number of trypan blue positive cells was negligible and always <2%.

Determination of Reactive Oxygen Species Production

ROS production has been monitored using the oxidation-sensitive probe dihydrorhodamine (DHR), which, upon oxidation, is converted into the fluorescent by-product rhodamine 123 [Royall and Ischiropoulos,

1993]. The formation of rhodamine 123 has been determined and quantified by means of image analysis-assisted fluorescence microscopy.

Cells were exposed to SMF for 4, 24, 48, and 72 h and 10 μ M DHR was added during the last 15 min of incubation. After accurate washings, cellular fluorescence was imaged using a Leica DMLB/DFC300F fluorescence microscope (Leica Microsystems, Wetzlar, Germany) equipped with an Olympus Color-viewIIIu CCD camera (Polyphoto, Milan, Italy). The light intensity and exposure settings were kept constant to allow quantitative comparisons of relative fluorescence intensity of cells between treatment groups. The exposure was limited to brief image acquisition intervals (<5 s) to minimize photooxidation of DHR. Fluorescence images (50 cells per sample from randomly selected fields) were digitally acquired and processed for fluorescence determination at the single cell level on a personal computer using the public domain program, Scion Image. Mean fluorescence values were determined by averaging the fluorescence of at least 50 cells/treatment condition/experiment.

Fast Halo Assay

The assay was carried out as previously described by Sestili et al. [2006]. Briefly, after the exposure (2, 4, 24, 48, and 72 h), the cells were resuspended at $4.0 \times 10^4/\mu$ l in ice-cold PBS containing 5 mM EDTA; this cell suspension was diluted with an equal volume of 2% low-melting agarose in PBS and immediately sandwiched between an agarose-coated slide and a coverslip. After complete gelling on ice, the coverslips were removed and the slides were immersed in NaOH 300 mM for 15 min at room temperature. Ethidium bromide (EtBr; 10 μ g/ml) was directly added to NaOH during the last 5 min of incubation. The slides were then washed and destained for 5 min in distilled water. The EtBr-labeled DNA was visualized using a Leica DMLB/DFC300F fluorescence microscope and the resulting images were digitally recorded on a PC and processed with an image analysis software (Scion Image). The amount of fragmented DNA diffusing out of the nuclear cage, that is, the extent of strand scission, was quantified by calculating the nuclear spreading factor, which represents the mean of the ratio between the total area of the halo and nucleus and that of the nucleus in scored cells from each experimental condition.

Isolation of Nucleic Acids

High molecular weight DNA and total RNA were isolated from about 3×10^5 HUVECs using the QIAamp DNA mini kit and the RNeasy mini kit (Qiagen, Milan, Italy), respectively, following the

manufacturer's instructions. A DNase (Ambion, Austin, TX) digestion step was performed on all the RNA samples before all subsequent reactions. The final concentration and quality of DNA and RNA were estimated both spectrophotometrically (DU-640; Beckman Instruments, Milan, Italy) at 260 nm, and by agarose gel electrophoresis.

Quantitative PCR (QPCR)

Two quantitative PCRs were performed through amplification of a long and a short fragment of mitochondrial DNA. Long PCR was performed using a GeneAmp PCR System 9700 thermocycler (PE Applied Biosystems, Milan, Italy). The reaction mixture contained 30 ng total DNA, 1.5 μ l buffer 1 \times , 200 μ M dNTPs, 0.5 μ M of each primer, and 0.3 μ l of Advantage 2 polymerase (EuroClone, Milan, Italy) in a final volume of 15 μ l. Primers Af–Ar (Table 1) were used to amplify a 16.2 kb fragment of the mitochondrial DNA (mtDNA).

PCR of the short fragment was performed to normalize the data obtained with the long PCR. We used primers ND1f and ND1r, which amplify a short fragment of the mitochondrial ND1 gene (NADH dehydrogenase complex 1), internal to the region amplified by Primers Af–Ar. The amplification of this short fragment reflects only the undamaged DNA due to the low probability of introducing lesions in small segments. The reaction mixture contained 4 ng total DNA, 1.5 μ l buffer 1 \times , 200 μ M dNTPs, 0.5 μ M of each primer, and 0.3 μ l of Advantage 2 polymerase. PCR parameters are reported in Table 2.

Previous experiments were set up for both long and ND1 PCRs in order to set up the reaction conditions

TABLE 1. Employed Primers

16.2 kb, mitochondrial fragment	
Af	5'-TGAGGCCAAATATCATTCTGAG-3'
Ar	5'-TTTCATCATGCGGAGATGTTGG-3'
100 bp, mitochondrial fragment	
ND1 f	5'-ACGCCATAAACTCTTCACCAAAG-3'
ND1 r	5'-TAGTAGAAGAGCGATGGTGAGAGCTA-3'
100 bp, nuclear fragment	
β -Actin f	5'-TGACTGGCCCGCTACCTCTT-3'
β -Actin r	5'-CGGCAGAAGAGAGAACCAGTGA-3'
128 bp, TFAM amplicon	
TFAM f	5'-TCACAATGGATAGGCACAGG-3'
TFAM r	5'-TGGCAGAAGTCCATGAGCT-3'
111 bp, 18S amplicon	
18S f	5'-TGACTCAACACGGGAAACCT-3'
18S r	5'-GCTCCACCAACTAAGAACG-3'
370 bp, mitochondrial fragment	
F ₂	5'-CCCCTCTAGAGCCCCTGTA-3'
R ₂	5'-GAGTGCTATAGGCGCTTGTC-3'

TABLE 2. Thermal Cycling Parameters in Long and ND1 PCRs

Cycles	Temperature (°C)	Time
16.2 kb mitochondrial fragment		
1×	95	1 min
24×	94	30 s
	68	16 min
1×	68	7 min
1×	4	∞
0.1 kb ND1 fragment		
1×	95	1 min
24×	94	30 s
	68	30 s
1×	68	7 min
1×	4	∞

and to work during the exponential phase. Lambda/*Hind* III DNA (from 0 to 200 ng in duplicate) was used to generate a standard curve.

The long PCR and ND1 amplification products were electrophoresed on 0.8% agarose/TBE gel, and 2% agarose/TBE gel stained with EtBr (0.3 µg/ml), respectively. The DNA concentration was calculated by densitometric analysis based on the standard curve using Quantity One Software 4.01 (Bio-Rad, Milan, Italy).

Four separate experiments were performed, in which two long and two ND1 PCRs were carried out per sample. The values utilized for statistical analyses were the relative amplifications, obtained by dividing long mtDNA/ND1 fluorescence values of the exposed samples with the long mtDNA/ND1 fluorescence values of the control (non-exposed) samples.

Detection of the Mitochondrial 4977 bp Common Deletion by a Standard PCR

To assess the presence of the common deletion [MITOMAP, 2009], which employs nucleotides from position 8469 to 13447, we have used two primers: F₂ and R₂ (Table 1), located at 8283 nt and 13610 nt of the complete *Homo sapiens* mitochondrial sequence (accession number NC_001807.4), respectively. These primers produce a 5347 bp amplicon from intact mitochondrial DNA and an amplicon of 370 bp in the presence of deletion (5347–4977). PCR reaction has been performed in a final volume of 25 µl containing 50 ng genomic DNA, 0.5 µM of F₂ and R₂ primers, 200 µM dNTPs, 2.5 µl of 10× buffer, 1.5 mM MgCl₂, and 1.5 U Taq DNA polymerase (Diateva, Fano, Italy). Reaction conditions were denaturation at 95 °C for 10 min followed by 30 cycles at 94 °C for 30 s, 59 °C for 30 s, and 72 °C for 30 s, with final extension at 72 °C for 7 min.

Mitochondrial DNA/Nuclear DNA Ratio

Real-time PCR was performed to determine the mtDNA/nDNA ratio by amplifying ND1 as the mtDNA, and β-actin as nDNA. Quantitative real-time PCR was performed using the Bio-Rad iCycler iQ Multicolor real-time PCR Detection System and a homemade amplification mix.

The reaction mix (25 µl final volume) consisted of 12.5 µl Mix (Hot-Start Taq; Qiagen), 50 ng/µl DNA template, 0.2× SYBR Green, and 0.3 µM of each primer (Table 1). The PCR conditions were carried out as follows: hot start at 95 °C for 10 min, then 40 cycles at 95 °C for 30 s and at 60 °C for 30 s. Threshold cycle (C_t) was determined on the linear phase of PCRs using the iCycler iQ Optical System Software version 3 (Bio-Rad). The specificity of the amplification products obtained has been confirmed by examining thermal denaturation plots, and by sample separation in a 3% DNA agarose gel. ND1 and β-actin gene copy numbers were determined by interpolating the threshold cycle (C_t) from standard curves. The standard curves and correlation coefficients were: $y = -3.198x + 26.959$, $R^2 = 0.984$ (ND1); $y = -3.219x + 38.897$, $R^2 = 0.997$ (β-actin). The ratios were obtained relating these mitochondrial and nuclear DNA quantities.

Expression Analysis of TFAM Gene for the Evaluation of Mitochondrial Biogenesis

The mitochondrial transcription factor A (TFAM) was selected as a target gene to evaluate mitochondrial biogenesis, and the ribosomal RNA 18S gene was selected as a housekeeping gene to normalize the results.

One microgram of DNase-treated total RNA was reverse transcribed using random hexamers and the Omniscript™ Reverse Transcriptase kit (Qiagen) following the manufacturer's instructions. Quantitative real-time PCR was performed using the Bio-Rad iCycler iQ Multicolor real-time PCR Detection System and the PCR conditions already described above. The sequence of the primers employed as target gene (TFAM) and internal standard (18S) is reported in Table 1. The specificity of the amplification products obtained was confirmed by examining thermal denaturation plots, and by sample separation in a 3% DNA agarose gel. The amount of the target transcript was related to that of the reference gene using the method described by Pfaffl [2001]. Each sample was tested in triplicate by quantitative PCR, and the samples obtained from at least six independent experiments were used to calculate the mean and standard error; the results were considered significant if *P*-values were <0.05.

Statistical Analysis

The statistical analysis was performed using GraphPad InStat version 3.00 (SxST.it, Milan, Italy). The variables between exposed and sham growths were compared using the unpaired Student's *t*-test. The differences between growths were considered significant if *P*-values were <0.05 .

RESULTS

In order to verify whether a 300 mT SMF has any effect on the viability of HUVECs, we performed the trypan blue exclusion assay on SMF-treated HUVECs; no significant differences were found between the control and exposed cells at the selected intervals of 4, 24, 48, and 72 h (Fig. 1).

Molecular assays were also performed to evaluate genomic integrity, either at the nuclear or mitochondrial level after exposure to the 300 mT SMF for increasingly longer periods (4, 24, 48, and 72 h). To determine nuclear integrity the fast halo assay was used. The fast halo assay revealed that SMF was capable of inducing detectable and significant damage on nDNA. Indeed, halos of fragmented DNA surrounding the nuclei of SMF-treated cells could be observed: a representative micrograph of cells exposed to SMFs for 4 h is shown in Figure 2C, while Figure 2B shows cells treated with H_2O_2 , included as a reference DNA-damaging agent [Sestili et al., 2006]; Figure 2A shows sham control cells. The bar graph of Figure 2 shows the data obtained by digitally analyzing the micrographs of HUVECs exposed for increasing time intervals to SMF; the extent of DNA breakage peaked at 4 h and progressively

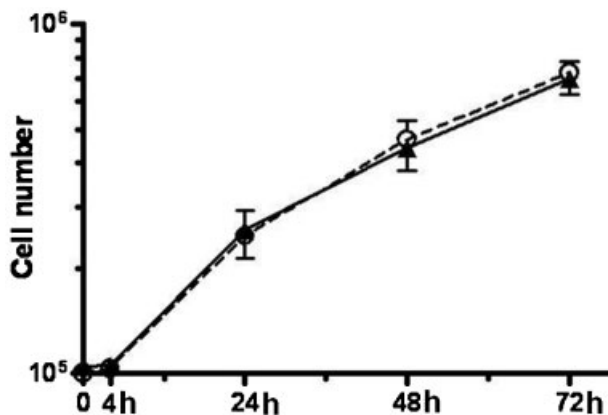


Fig. 1. Effect of static magnetic field exposure on HUVEC growth. Cells were grown in the absence (circles) or presence (triangles) of a 300 mT static magnetic field. Each point represents the mean \pm SEM from five separate determinations, each performed in duplicate.

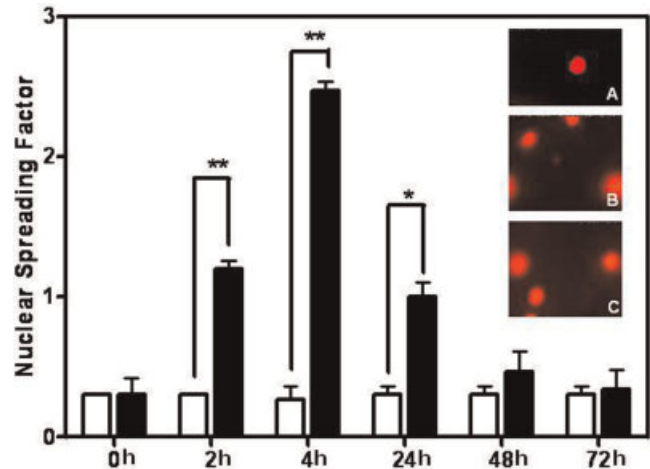


Fig. 2. Effect of exposure on HUVECs as assessed with the fast halo assay. HUVECs were exposed to 0 (open columns) or a 300 mT (solid columns) static magnetic field. Representative micrographs of HUVECs processed for DNA damage with the fast halo test are also shown: **Panel A**: Control cells; **panel B**: Cells treated with 0.1 mM H_2O_2 for 30 min, included as positive control; **panel C**: 4 h SMF-exposed cells. Each point represents the mean \pm SEM from four separate determinations, each performed in duplicate. **P* < 0.05 and ***P* < 0.01 (unpaired Student's *t*-test) SMF-treated versus control cells.

decreased at longer SMF exposure times. At 48 and 72 h no significant difference between exposed and control cultures could be determined.

Mitochondrial DNA integrity was investigated by QPCR and by the detection of 4977 deletion, also known as the common deletion. QPCR analyses showed a reduced mtDNA amplification yield only after the shortest SMF exposure time (4 h) and no significant difference at the remaining exposure times, compared to control (Fig. 3).

The common deletion is the most extensively studied in mtDNA and is generally used as an indicator of tissue deterioration in aging and bioenergetics. This deletion was never detected under the conditions presented here (Fig. 4) and for this reason we did not perform any quantitative analyses.

Four-hour SMF exposure (the time point associated with the peak of DNA breakage) also caused a marked oxidation of DHR into its fluorescent derivative, rhodamine 123 (Fig. 5). Interestingly, this phenomenon is known to depend on increased intracellular generation of ROS [Palomba et al., 2000]. No significant difference was observed by this assay for the remaining exposure times.

Further biomolecular investigations were carried out in order to evaluate the possible effects of this MF on mitochondrial content and biogenesis. The mtDNA/nDNA ratio and gene expression analysis of a target

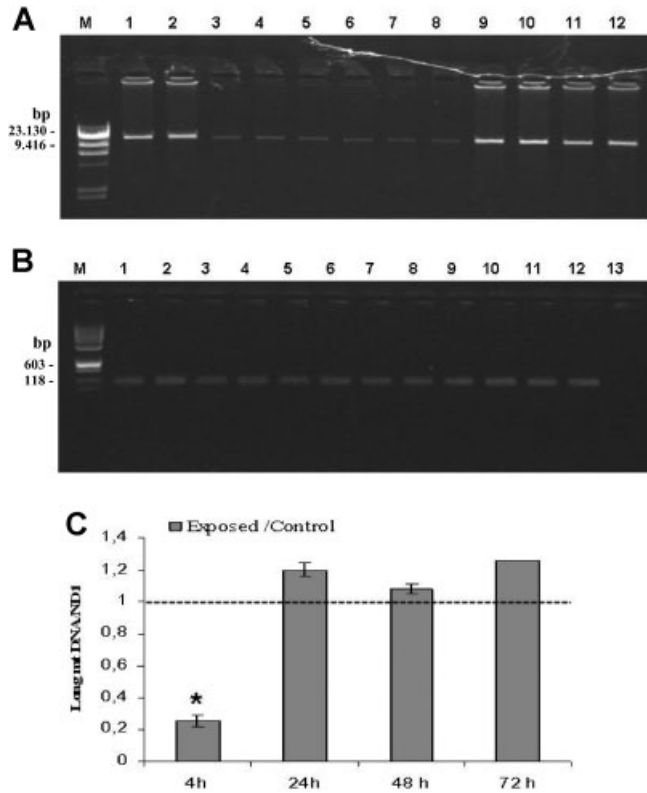


Fig. 3. Quantitative PCR. **A:** Example of electrophoretic pattern of long PCR showing the effect of a 300 mT static magnetic field on mitochondrial DNA. **Lane M:** DNA molecular weight Lambda/*Hind* III; **lanes 1, 2, 9–12:** amplified products from 4 h control cells; **lanes 3–8:** amplified products from 4 h exposed cells. **B:** Electrophoretic pattern of the same DNA samples amplified with ND1 primers, internal to the long amplification. **Lane M:** DNA molecular weight X174/*Hae* III; **lanes 1–6:** amplified products from four control cells; **lanes 7–12:** amplified products from 4 h exposed cells; **lane 13:** no DNA; **C:** Densitometric analysis of the electrophoretic profiles of mitochondrial long PCR/ND1 from HUVECs grown for 4, 24, 48, and 72 h in the presence or absence of the field. The amplification yield of exposed samples was calculated comparing treated samples to control (dashed line). Data are expressed as the mean \pm SEM of at least four separate experiments in which two long and two ND1 PCRs were carried out per sample. Unpaired Student's *t*-test was performed. **P* < 0.05 when controls and exposed cells were compared.

gene of the mitochondrial biogenesis were performed. Mitochondrial DNA content was evaluated performing real-time PCR of mitochondrial ND1 gene normalized with nuclear β -actin gene. This mtDNA/nDNA analysis showed a reduction of mitochondrial DNA after 4 h exposure, an increase after 24 h, and no significant difference in the remaining experimental trials (Fig. 6). Data obtained at 4 h exposure with this assay were surprising, since we did not expect significant changes in the mitochondrial DNA content. Finally, gene expression analysis of TFAM showed a statistically

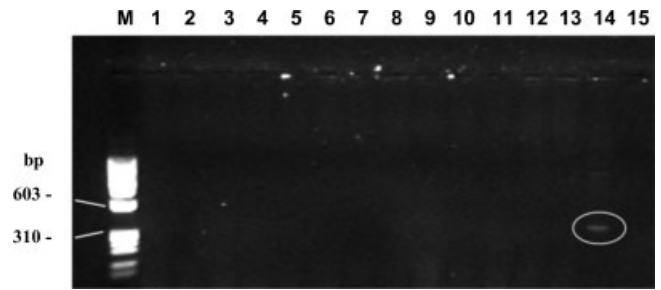


Fig. 4. Electrophoretic pattern for the detection of a 370 bp amplicon, marker of the common deletion. **Lane M:** DNA molecular weight X174/*Hae* III. **Lanes 1–4:** amplification from 4 h control cells; **lanes 5–8:** amplification from 4 h exposed cells; **lanes 9–10:** amplification from 24 h control cells; **lanes 11–13:** amplification from 24 h exposed cells; **lane 14:** positive control from DNA of a patient with colorectal cancer; **lane 15:** no DNA.

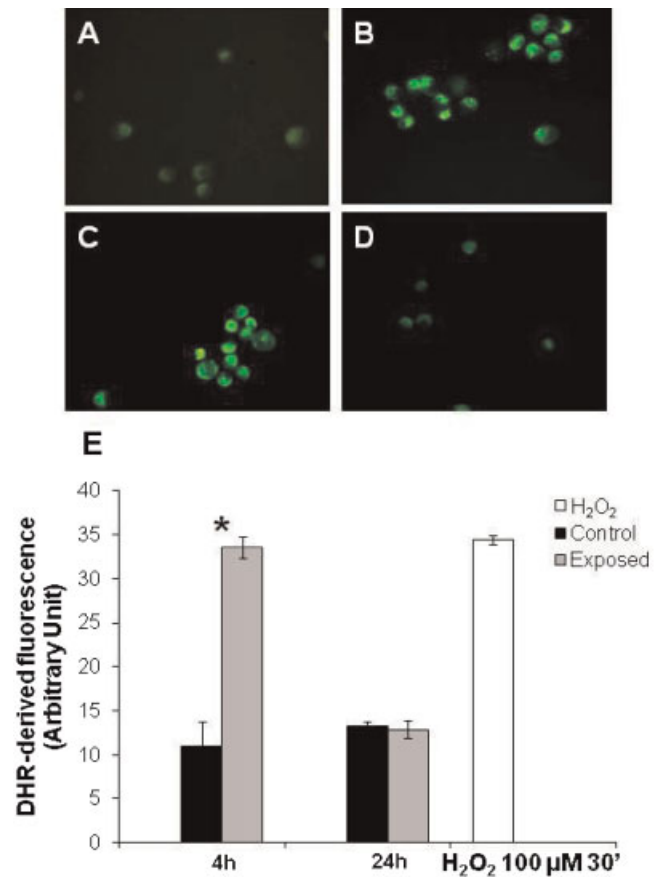


Fig. 5. DHR fluorescence observed in HUVEC. **Panel A:** 4 h control cells; **panel B:** cells treated with 100 μ M H₂O₂; **panel C:** 4 h exposed cells; **panel D:** 24 h control cells; **panel E:** densitometric image analysis.

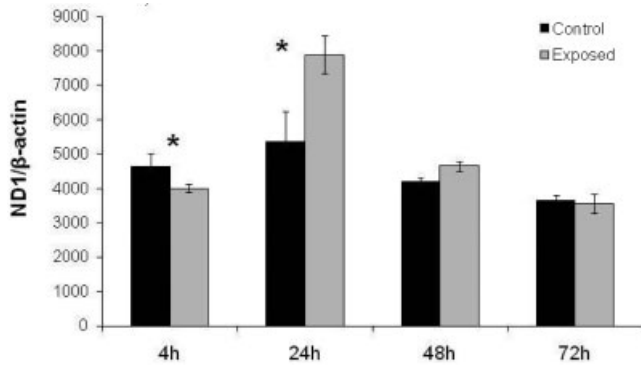


Fig. 6. Determination of mtDNA/nDNA ratio as ND1/β-actin by real-time PCR. Data are expressed as the mean ± SEM of four experiments; all samples were analyzed in triplicate. Unpaired Student's *t*-test was performed. * $P < 0.05$ when controls and exposed cells were compared.

significant increase, though not a dramatic increase, only in cells exposed for 24 h (Fig. 7).

DISCUSSION

Recent studies have shown that SMFs give rise to intracellular and extracellular changes [Miyakoshi, 2005; Amara et al., 2007], the likely consequences of an initial effect on the properties of plasma membranes [Rosen, 2003]. Little is known about how this field affects the mitochondria [Schmitz et al., 2004; Dini et al., 2009], the organelles now considered the brain of the cell. We carried out the present study chiefly to fill the existing gaps in the literature in this area.

Using HUVECs we first found that exposure to a 300 mT SMF had no significant effect on cell growth. It is generally accepted that the effect of SMF exposure alone may vary greatly, essentially depending on the cell type and intensity of the exposure [Miyakoshi,

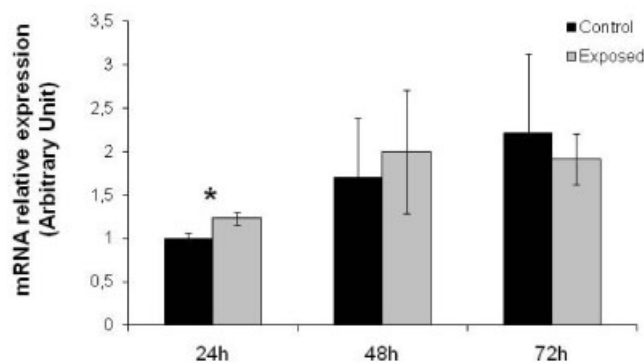


Fig. 7. Quantitative analyses of TFAM by real-time PCR. Data are expressed as the mean ± SEM; all samples were analyzed in triplicate. Unpaired Student's *t*-test was performed; P -values were < 0.05 .

2005]. Indeed, some studies have reported that repetitive SMF exposure has no effect on cell growth rate, whereas others have shown that SMF alone alters cell proliferation/cell death balance. Wiskirchen et al. [1999], for example, found that repetitive exposure to a SMF of 1.5 T exerted no effects on proliferation of human fetal lung fibroblast cells, while Raylman et al. [1996] reported that prolonged exposure to a 7 T SMF produced a reduction in viable cell number in melanoma, ovarian carcinoma, and lymphoma cell lines. Buemi et al. [2001] observed a gradual decrease in apoptosis and proliferation, and a gradual increase in necrosis in renal cells exposed to 0.5 mT SMF, compared to the control group.

However, our major interest was to analyze the effects of SMFs on the nucleus and mitochondria. Nuclear DNA damage induced by SMFs has already been investigated using the comet assay [Miyakoshi, 2005; Amara et al., 2007], but nothing is available regarding the effects on mtDNA integrity and little on mitochondria involvement [Gorczyńska and Węgrzynowicz, 1991; Dini et al., 2009]. This work represents one of the first investigations in this area.

We found significant DNA damage at both the nuclear and mitochondrial levels after 4 h of exposure (Figs. 2, 3, and 6) and only at the nuclear level after 24 h (Fig. 2). The absence of the common deletion in our system suggests that a 300 mT SMF does not induce this kind of damage in mitochondrial DNA.

Data obtained by real-time PCR using the ratio mitochondrial DNA/nuclear DNA showed a reduction in mitochondrial DNA content (Fig. 6), which was unexpected at 4 h of exposure. We had assumed possible mitochondrial DNA damage but not a significant reduction of its content. This real-time result led us to interpret QPCR data at 4 h of exposure as follows: the sharp reduction of mt-amplified DNA in the exposed samples compared to controls may be due to either the presence of lesions or to the reduction of mtDNA target. However, in general, both the lesions and the reduction of mtDNA content at 4 h of exposure might be a consequence of the increased production of ROS, which were significantly highlighted at the same exposure time using the sensitive probe, DHR (Fig. 5). Since ROS are primarily produced in the mitochondria, they mainly damage mtDNA which is located in the mitochondrial matrix. Moreover, the effects of SMFs on cellular kinetics of free radical-related cellular processes have already been reported in literature [Flipo et al., 1998; Katsir et al., 1998; Danielyan and Ayrapetyan, 1999; Fanelli et al., 1999; Eveson et al., 2000; Gray et al., 2000; Buemi et al., 2001; Potenza et al., 2004; Amara et al., 2006, 2007; Chater et al., 2006]. It was also proposed that SMFs initiate an iron-

dependent free radical generation process within target cells, which can lead to genotoxic effects and/or cell death, and it is documented that treatment with trace amounts of ferrous ions in the cell culture medium and exposure to a SMF increased DNA damage [Zmyslony et al., 2000; Jajte et al., 2002; Miyakoshi, 2006]. Hence, one could speculate that the SMF primarily affects cells with high rates of iron intake such as proliferating cells, virus-infected cells, and cells with high metabolic rates, for example, brain cells. The data on DNA integrity with increasing SMF time exposure (24, 48, and 72 h) indicate the progressive recruitment of repair processes, both at the nuclear and mitochondrial level. Furthermore, the return to normal levels of ROS, recorded from 24 h onward (Fig. 5), could point to the cell's ability to adapt to a new condition, the exposure to the field.

The significantly increased ratios of mtDNA/nDNA (Fig. 6) and the higher expression level of TFAM gene after 24 h of exposure (Fig. 7) suggest that a 300 mT SMF may stimulate mitochondrial biogenesis. This is an extremely complex process because mitochondria are composed of proteins derived from both nuclear and mitochondrial genomes. The molecular processes involved in this pathway were not investigated in the present work. However, some events which occur after SMF exposure are similar to the mitochondrial biogenesis induced in skeletal muscle by physical exercise [Chabi et al., 2005; Hood et al., 2006; Yan et al., 2007; Arany, 2008; Hood, 2009], for example, the intracellular Ca^{2+} increase and the over-expression of specific transcription factors known to play a pivotal role, such as TFAM. Calcium ion fluxes and modulation of intracellular concentration are of particular interest in many biological functions due to ion activation of signal pathways, and it is well known that MFs induce intracellular Ca^{2+} changes [Flipo et al., 1998; Fanelli et al., 1999; Chionna et al., 2005; Tenuzzo et al., 2006; Belton et al., 2009]. Moreover, TFAM is a mitochondrial transcription factor that is a key activator of mitochondrial transcription, as well as a participant in mitochondrial genome replication. Studies in mice have demonstrated that this gene product is required to regulate the mitochondrial genome copy number [Tominaga et al., 1992; Chionna et al., 2005; Kang and Hamasaki, 2005; Kang et al., 2007; Belton et al., 2009].

Structural changes in hepatocyte mitochondria associated with an increase in the activities of the mitochondrial respiratory enzymes, NADH dehydrogenase, succinic dehydrogenase, and cytochrome oxidase, were found by Gorczynska and Wegrzynowicz [1991] in rats exposed to MFs of 10^{-3} and 10^{-2} T for 1 h. Evidence of increased mtDNA synthesis after MF exposure has been already reported by Schmitz et al.

[2004] in two cell types of renal segmentation. An increase in the number of mitochondria was also found by Dini et al. [2009] when differentiation of U937 cells was induced by a 6 mT SMF. Our results are in line with these three studies, suggesting that the SMF stimulates mitochondrial biogenesis.

It could be hypothesized that when redox balance is altered, as it is under SMF exposure, mitochondrial biogenesis represents a cellular pro-survival factor against oxidative stress.

In conclusion, the results reported herein suggest that a 300 mT SMF applied to HUVECs does not cause permanent injuries to nDNA and mtDNA. In fact, the injuries induced by SMF after 4 h of exposure are rapidly and definitively repaired in trials with increasingly longer SMF exposure. Hence, although further studies will be needed, the genotoxic relevance of these lesions seems to be negligible. Furthermore, it is likely that these lesions are not cytotoxically relevant, since no cell demise or growth arrest was observed in SMF-exposed HUVECs.

Another noteworthy effect promoted by SMF and described in this study consists in the stimulation of mitochondrial DNA synthesis, and in the modulation of the expression pattern of one the main genes involved in mitochondrial biogenesis. These findings may contribute to future research on the use of SMFs in medical applications.

REFERENCES

- Amara S, Abdelmelek H, Garrel C, Guiraud P, Douki T, Ravanat JL, Favier A, Sakly M, Ben RK. 2006. Effects of subchronic exposure to static magnetic field on testicular function in rats. *Arch Med Res* 37(8):947–952.
- Amara S, Douki T, Ravanat JL, Garrel C, Guiraud P, Favier A, Sakly M, Ben RK, Abdelmelek H. 2007. Influence of a static magnetic field (250 mT) on the antioxidant response and DNA integrity in THP1 cells. *Phys Med Biol* 52(4):889–898.
- Arany Z. 2008. PGC-1 coactivators and skeletal muscle adaptations in health and disease. *Curr Opin Genet Dev* 18(5):426–434.
- Belton M, Prato FS, Rozanski C, Carson JJ. 2009. Effect of 100 mT homogeneous static magnetic field on $[\text{Ca}^{2+}]_i$ response to ATP in HL-60 cells following GSH depletion. *Bioelectromagnetics* 30(4):322–329.
- Buemi M, Marino D, Di PG, Floccari F, Senatore M, Aloisi C, Grasso F, Mondio G, Perillo P, Frisina N, Corica F. 2001. Cell proliferation/cell death balance in renal cell cultures after exposure to a static magnetic field. *Nephron* 87(3):269–273.
- Cairo P, Greenebaum B, Goodman E. 1998. Magnetic field exposure enhances mRNA expression of sigma 32 in *E. coli*. *J Cell Biochem* 68(1):1–7.
- Chabi B, Adhietty PJ, Ljubovic V, Hood DA. 2005. How is mitochondrial biogenesis affected in mitochondrial disease? *Med Sci Sports Exerc* 37(12):2102–2110.
- Chater S, Abdelmelek H, Douki T, Garrel C, Favier A, Sakly M, Ben RK. 2006. Exposure to static magnetic field of pregnant rats

- induces hepatic GSH elevation but not oxidative DNA damage in liver and kidney. *Arch Med Res* 37(8):941–946.
- Chionna A, Tenuzzo B, Panzarini E, Dwikat MB, Abbro L, Dini L. 2005. Time dependent modifications of Hep G2 cells during exposure to static magnetic fields. *Bioelectromagnetics* 26(4):275–286.
- Danielyan AA, Ayrapetyan SN. 1999. Changes of hydration of rats' tissues after in vivo exposure to 0.2 Tesla steady magnetic field. *Bioelectromagnetics* 20(2):123–128.
- Dini L, Abbro L. 2005. Bioeffects of moderate-intensity static magnetic fields on cell cultures. *Micron* 36(3):195–217.
- Dini L, Dwikat M, Panzarini E, Vergallo C, Tenuzzo B. 2009. Morphofunctional study of 12-O-tetradecanoyl-13-phorbol acetate (TPA)-induced differentiation of U937 cells under exposure to a 6 mT static magnetic field. *Bioelectromagnetics* 30(5):352–364.
- Eveson RW, Timmel CR, Brocklehurst B, Hore PJ, McLauchlan KA. 2000. The effects of weak magnetic fields on radical recombination reactions in micelles. *Int J Radiat Biol* 76(11):1509–1522.
- Fanelli C, Coppola S, Barone R, Colussi C, Gualandi G, Volpe P, Ghibelli L. 1999. Magnetic fields increase cell survival by inhibiting apoptosis via modulation of Ca²⁺ influx. *FASEB J* 13(1):95–102.
- Flipo D, Fournier M, Benquet C, Roux P, Le BC, Pinsky C, LaBella FS, Krzystyniak K. 1998. Increased apoptosis, changes in intracellular Ca²⁺, and functional alterations in lymphocytes and macrophages after in vitro exposure to static magnetic field. *J Toxicol Environ Health A* 54(1):63–76.
- Franco G, Perduri R, Murolo A. 2008. Health effects of occupational exposure to static magnetic fields used in magnetic resonance imaging: A review. *Med Lav* 99(1):16–28.
- Gorzynska E, Wegrzynowicz R. 1991. Structural and functional changes in organelles of liver cells in rats exposed to magnetic fields. *Environ Res* 55(2):188–198.
- Gray JR, Frith CH, Parker JD. 2000. In vivo enhancement of chemotherapy with static electric or magnetic fields. *Bioelectromagnetics* 21(8):575–583.
- Henry SL, Concannon MJ, Yee GJ. 2008. The effect of magnetic fields on wound healing: Experimental study and review of the literature. *Eplasty* 8:40.
- Hong FT. 1995. Magnetic field effects on biomolecules, cells, and living organisms. *Biosystems* 36(3):187–229.
- Hood DA. 2009. Mechanisms of exercise-induced mitochondrial biogenesis in skeletal muscle. *Appl Physiol Nutr Metab* 34(3):465–472.
- Hood DA, Irrcher I, Ljubicic V, Joseph AM. 2006. Coordination of metabolic plasticity in skeletal muscle. *J Exp Biol* 209(Pt 12):2265–2275.
- Ishizaki Y, Horiuchi S, Okuno K, Ano T, Shoda M. 2001. Twelve hours exposure to inhomogeneous high magnetic field after logarithmic growth phase is sufficient for drastic suppression of *Escherichia coli* death. *Bioelectrochemistry* 54(2):101–105.
- Jajte J, Grzegorzczak J, Zmyslony M, Rajkowska E. 2002. Effect of 7 mT static magnetic field and iron ions on rat lymphocytes: Apoptosis, necrosis and free radical processes. *Bioelectrochemistry* 57(2):107–111.
- Kang D, Hamasaki N. 2005. Mitochondrial transcription factor A in the maintenance of mitochondrial DNA: Overview of its multiple roles. *Ann N Y Acad Sci* 1042:101–108.
- Kang D, Kim SH, Hamasaki N. 2007. Mitochondrial transcription factor A (TFAM): Roles in maintenance of mtDNA and cellular functions. *Mitochondrion* 7(1–2):39–44.
- Karasek M, Lerchl A. 2002. Melatonin and magnetic fields. *Neuro Endocrinol Lett* 23(Suppl):184–187.
- Katsir G, Parola AH. 1998. Enhanced proliferation caused by a low frequency weak magnetic field in chick embryo fibroblasts is suppressed by radical scavengers. *Biochem Biophys Res Commun* 252(3):753–756.
- Katsir G, Baram SC, Parola AH. 1998. Effect of sinusoidally varying magnetic fields on cell proliferation and adenosine deaminase specific activity. *Bioelectromagnetics* 19(1):46–52.
- Kheifets LI. 2001. Electric and magnetic field exposure and brain cancer: A review. *Bioelectromagnetics* 22(Suppl 5):S120–S131.
- MITOMAP. 2009. Reported mtDNA deletions. <http://www.mitomap.org/MITOMAP/DeletionsSingle> (last accessed April 11, 2009).
- Miyakoshi J. 2005. Effects of static magnetic fields at the cellular level. *Prog Biophys Mol Biol* 87(2–3):213–223.
- Miyakoshi J. 2006. The review of cellular effects of a static magnetic field. *Sci Technol Adv Mat* 7:7305–7307.
- Nursal TZ, Bal N, Anarat R, Colakoglu T, Noyan T, Moray G, Haberal M. 2006. Effects of a static magnetic field on wound healing: Results in experimental rat colon anastomoses. *Am J Surg* 192(1):76–81.
- Okano H. 2008. Effects of static magnetic fields on blood pressure in animals and humans. *Curr Hypertens Rev* 4(1):463–472.
- Okano H, Onmori R, Tomita N, Ikada Y. 2006. Effects of a moderate-intensity static magnetic field on VEGF-A stimulated endothelial capillary tubule formation in vitro. *Bioelectromagnetics* 27(8):628–640.
- Palomba L, Sestili P, Guidarelli A, Sciorati C, Clementi E, Fiorani M, Cantoni O. 2000. Products of the phospholipase A(2) pathway mediate the dihydrorhodamine fluorescence response evoked by endogenous and exogenous peroxynitrite in PC12 cells. *Free Radic Biol Med* 29(8):783–789.
- Pfaffl MW. 2001. A new mathematical model for relative quantification in real-time RT-PCR. *Nucleic Acids Res* 29(9):e45.
- Potenza L, Ubaldi L, De SR, De BR, Cucchiari L, Dachà M. 2004. Effects of a static magnetic field on cell growth and gene expression in *Escherichia coli*. *Mutat Res* 561(1–2):53–62.
- Raylman RR, Clavo AC, Wahl RL. 1996. Exposure to strong static magnetic field slows the growth of human cancer cells in vitro. *Bioelectromagnetics* 17(5):358–363.
- Rosen AD. 2003. Mechanism of action of moderate-intensity static magnetic fields on biological systems. *Cell Biochem Biophys* 39(2):163–173.
- Royall JA, Ischiropoulos H. 1993. Evaluation of 2',7'-dichlorofluorescein and dihydrorhodamine 123 as fluorescent probes for intracellular H₂O₂ in cultured endothelial cells. *Arch Biochem Biophys* 302(2):348–355.
- Rumbaut RE, Mirkovic D. 2008. Magnetic therapy for edema in inflammation: A physiological assessment. *Am J Physiol Heart Circ Physiol* 294(1):H19–H20.
- Sabo J, Mirossay L, Horovcak L, Sarissky M, Mirossay A, Mojzic J. 2002. Effects of static magnetic field on human leukemic cell line HL-60. *Bioelectrochemistry* 56(1–2):227–231.
- Schmitz C, Keller E, Freuding T, Silny J, Korr H. 2004. 50-Hz magnetic field exposure influences DNA repair and mitochondrial DNA synthesis of distinct cell types in brain and kidney of adult mice. *Acta Neuropathol* 107(3):257–264.
- Sestili P, Martinelli C, Stocchi V. 2006. The fast halo assay: An improved method to quantify genomic DNA strand breakage at the single-cell level. *Mutat Res* 607(2):205–214.

- Strelczyk D, Eichhorn ME, Luedemann S, Brix G, Dellian M, Berghaus A, Strieth S. 2009. Static magnetic fields impair angiogenesis and growth of solid tumors in vivo. *Cancer Biol Ther* 8:18.
- Tenuzzo B, Chionna A, Panzarini E, Lanubile R, Tarantino P, Di Jeso B, Dwikat M, Dini L. 2006. Biological effects of 6 mT static magnetic fields: A comparative study in different cell types. *Bioelectromagnetics* 27(7):560–577.
- Tominaga K, Akiyama S, Kagawa Y, Ohta S. 1992. Upstream region of a genomic gene for human mitochondrial transcription factor 1. *Biochim Biophys Acta* 1131(2):217–219.
- Wiskirchen J, Groenewaeler EF, Kehlbach R, Heinzelmann F, Wittau M, Rodemann HP, Claussen CD, Duda SH. 1999. Long-term effects of repetitive exposure to a static magnetic field (1.5 T) on proliferation of human fetal lung fibroblasts. *Magn Reson Med* 41(3):464–468.
- Xu S, Tomita N, Ohata R, Yan Q, Ikada Y. 2001. Static magnetic field effects on bone formation of rats with an ischemic bone model. *Biomed Mater Eng* 11(3):257–263.
- Yan Z, Li P, Akimoto T. 2007. Transcriptional control of the Pgc-1alpha gene in skeletal muscle in vivo. *Exerc Sport Sci Rev* 35(3):97–101.
- Zmyslony M, Palus J, Jajte J, Dziubaltowska E, Rajkowska E. 2000. DNA damage in rat lymphocytes treated in vitro with iron cations and exposed to 7 mT magnetic fields (static or 50 Hz). *Mutat Res* 453(1):89–96.